

Massive MIMO Array Design with High Isolation by Using Decoupling Cavity

Luo, Shengyuan; Pedersen, Gert Frølund; Zhang, Shuai

Published in:

I E E E Transactions on Circuits and Systems. Part 2: Express Briefs

DOI (link to publication from Publisher):

[10.1109/TCSII.2022.3216394](https://doi.org/10.1109/TCSII.2022.3216394)

Creative Commons License

Unspecified

Publication date:

2023

Document Version

Accepted author manuscript, peer reviewed version

[Link to publication from Aalborg University](#)

Citation for published version (APA):

Luo, S., Pedersen, G. F., & Zhang, S. (2023). Massive MIMO Array Design with High Isolation by Using Decoupling Cavity. *I E E E Transactions on Circuits and Systems. Part 2: Express Briefs*, 70(3), 974-978. <https://doi.org/10.1109/TCSII.2022.3216394>

General rights

Copyright and moral rights for the publications made accessible in the public portal are retained by the authors and/or other copyright owners and it is a condition of accessing publications that users recognise and abide by the legal requirements associated with these rights.

- Users may download and print one copy of any publication from the public portal for the purpose of private study or research.
- You may not further distribute the material or use it for any profit-making activity or commercial gain
- You may freely distribute the URL identifying the publication in the public portal -

Take down policy

If you believe that this document breaches copyright please contact us at vbn@aub.aau.dk providing details, and we will remove access to the work immediately and investigate your claim.

Massive MIMO Array Design with High Isolation by Using Decoupling Cavity

Shengyuan Luo, Gert Frølund Pedersen, *IEEE Senior Member*, Shuai Zhang, *IEEE Senior Member*

Abstract—This letter proposes an isolation enhancement method for massive multiple-input multiple-output arrays using decoupling cavities (DC). The proposed DC is made of a pure Polypropylene (PP) board, and an air cavity is engraved on it. The DC has high transmission in the normal direction and a high insertion loss in the tangential direction of the arrays, respectively. The DC operates with a broadband response due to the low dielectric constant of the substrate. An example of a 4×4 array with an inter-element distance around half wavelength is designed to verify the proposed isolation enhancement method. The triple-layers stacked DC are employed seamlessly above the array. The isolation of the array was enhanced to 24 dB within the bandwidth of 4.21-4.79 GHz. At the same time, the radiation characteristics of the arrays before and after loading the DC basically keep consistent.

Index Terms—Decoupling cavity (DC), isolation enhancement, massive multiple-input multiple-output (MIMO) antenna arrays.

I. INTRODUCTION

THIS massive multiple-input multiple-output (MIMO) systems have been widely used in current and future wireless communications [1-3]. During the implementation progress, the mutual coupling of the array seriously degrades the antenna performance, such as signal-to-noise ratio, active voltage standing wave ratio (VSWR), impedance match, and channel capacity [4-6]. Thus, researchers have paid much effort to the isolation enhancement for massive MIMO arrays.

The isolation enhancement in terms of the surface waves coupling suppression includes electromagnetic bandgap structure (EBG), defected ground structure, parasitic structures, metamaterial, and so on [7-11]. Typically, the mentioned technologies need a relatively larger space to employ the decoupling structure between the array elements. Therefore, it is inapplicable for massive MIMO arrays with a compact layout. Regarding reducing the space waves coupling, a metasurface and a dielectric block for two-element were proposed in [12] and [13], respectively. However, they face some difficulties for massive MIMO arrays with more intricate coupling paths.

For the massive MIMO arrays, a phase compensation method-based array decoupling surface (ADS) was developed in [14] to simultaneously reduce the couplings between

adjacent co-polarized antenna elements with diversified phase legging, but the issue of high design complexity cannot be avoided. Transmission-line-based decoupling technology was proposed in [15], yet it worked with a narrow bandwidth response. Reference [16] presented a decoupling method of a near-field resonator for large-scale arrays, but it is difficult to be extended to dual-polarized arrays due to the feature of asymmetry. Reference [17] introduced a decoupling ground to make the mutual coupling between the free space and the ground out of phase. However, the distance between the array elements is around 0.62λ . Reference [18] proposed an embeddable structure for reducing mutual coupling in a 3×3 MIMO array, but the worst co-polarized mutual isolation is only 20 dB. Reference [19] proposed a decoupling method of dielectric superstrate. But it can only be used in dual-element and single polarized array.

This letter proposes a scheme for implementing a massive MIMO array with high isolation by utilizing DC. The distance between the array elements is around half wavelength. The proposed DC has high transmission in the normal direction and high insertion loss in the tangential direction of the array. So that the space waves can normally propagate in the normal direction, and the propagation of the space waves along the parallel direction of the arrays can be suppressed. Three-layer stacked DC are mounted seamlessly above the reference array to enforce the decoupling effect. The proposed decoupling mechanism, an example of a 4×4 array, and antenna performance is described.

II. THE EXAMPLE OF 4×4 ARRAY WITH DC

A. Decoupling scheme of the DC

The space wave coupling dominates for the array with an inter-element distance of around half wavelength. For any array element of the massive MIMO array, the space waves are radiated in all directions in space. Therefore, the massive MIMO array has complicated coupling paths. But most coupling energy is radiated to the adjacent and non-adjacent elements in linear and diagonal directions, where the space coupling in E-plane and H-plane play a decisive role. Correspondingly, the total decoupling performance can be carried out by reducing the space coupling in the E-plane or E-plane of the array with an inter-element distance of half-

This work was supported in part by the Huawei project of “mm Wave Decoupling Array”. (Corresponding author: Shuai Zhang)

Shengyuan Luo, Gert Frølund Pedersen, and Shuai Zhang are with the Antenna, Propagation and Millimeter-Wave Systems (APMS) Section, Aalborg

University, 9220 Aalborg, Denmark (e-mail: shengyuanl@es.aau.dk; gfp@es.aau.dk; sz@es.aau.dk).

wavelength. Fig. 1 presents the decoupling schematic diagrams of the DC for massive MIMO arrays. Our goal is to design a decoupling structure that can suppress the propagation of the space waves along the tangential direction of arrays. In this paper, a DC is designed and loaded on the top surface of the original array. Here, the DC performs high transmission in the normal direction and high insertion loss in the tangential direction of the array. Consequently, the space coupling component attenuates when it propagates along the x-direction, which leads to strong energy insertion loss. Finally, the space waves coupling can be suppressed. Meanwhile, the DC has a perfect impedance matching with the arrays due to high transmission in the normal direction.

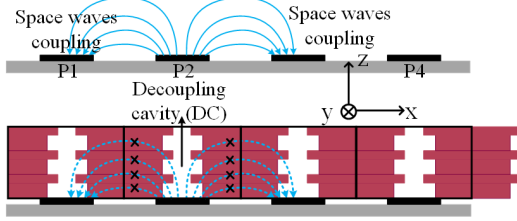


Fig. 1. Decoupling schematic of the massive MIMO arrays with the DCs.

B. The of 4×4 array antenna design

Fig. 2 depicts the geometries and specific dimensions of the 4×4 dual-polarized and wideband massive MIMO array with the proposed DC. Fig. 2 (a) and (b) present the decoupled 4×4 array and the detailed structure of the DC, respectively. Fig. 2 (b) shows the reference array and the prototype.

Each DC unit consists of two layers of pure PP (polypropylene) boards, where the permittivity of PP is around 2.2. Two air cavities are etched on the PP boards to adjust the insertion loss. The first layer has a thickness of 3 mm with a smaller square air cavity, while the second layer has a thickness of 6 mm with a larger square air cavity. Here, the period of the DC is set as the inter-element distance between the array elements. The extra weight of the adding material is 600 g in total. In the applications, it is also easy to find some other light materials with the permittivity of around 2.2, so the weight can be much further reduced.

Based on the decoupling concept of DC, an actual example of a 4×4 dual-polarized and wideband massive MIMO array with the proposed DC is carried out. The array element comprises two-layer stacked microstrip antennas to broaden the bandwidth. The metal patches are printed on the RO 4350B substrates with a permittivity of 3.66 and a loss tangent of 0.002. Four slots are etched on the metal patches of the bottom and top microstrip antenna to reduce the coupling level between two feed ports of the array elements themselves. In addition, the slots on the bottom and top antennas have the same size. The antennas are fed by the coaxial cables, where the inner conductors and the outer conductors of the cables connect with metal patches and the common ground of the bottom antennas, respectively. A PP board with air cavities above the feed point is inserted between the bottom and top substrates. Then, the DC is mounted on the top surface of the array to reduce the coupling. The optimized dimensions of the decoupled array are listed in TABLE I.

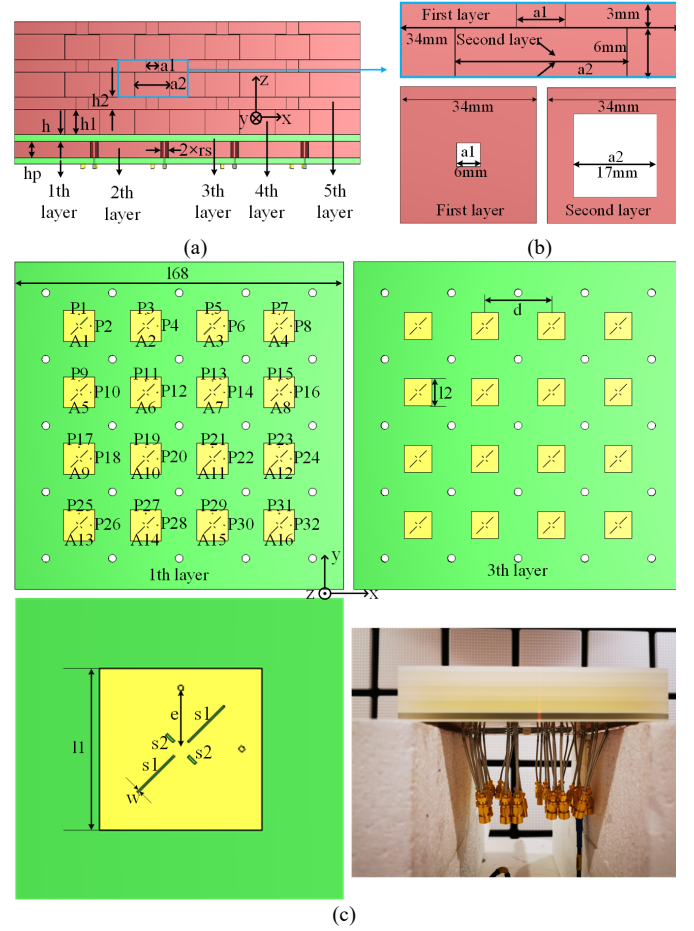


Fig. 2. Geometry and specific dimensions of the array with the proposed DC and the prototype: (a) the decoupled 4×4 array, (b) the detailed structure and specific dimensions of the DC, (c) the reference array and the prototype.

TABLE I
DIMENSIONS OF THE DECOUPLED ARRAY

Parameters	l	$l1$	$l2$	d	e
Values(mm)	168	8	7	34	6.8
parameters	rs	$a1$	$a2$	h	hp
Values(mm)	2	6	17	1.524	4
parameters	$s1$	$s1$	$h1$	$h2$	
Values(mm)	5	2	6	3	

C. The antenna performance

For the 4×4 arrays, the inner loop array elements have a more comprehensive coupling type with the other array elements. Additionally, since the symmetry feature of the arrays, element A6 has similar coupling paths with the other inner loop elements. Therefore, the mutual coupling between A6 and other elements can represent all the coupling types. The mutual coupling in this paper refers to the port-to-port mutual coupling. Here, we select the S-parameter of feed port P11 of the arrays before and after employing the DC and give it in Fig. 3. Notably, the $S_{11,11}$ and $S_{12,11}$ represent the reflection coefficient and the orthogonal polarized coupling level of the array elements themselves. The $S_{1,11}$, $S_{5,11}$, $S_{17,11}$, and $S_{21,11}$ represent the mutual coupling between the adjacent elements in the diagonal directions. The $S_{3,11}$, $S_{19,11}$, and $S_{27,11}$ denote the mutual coupling between the adjacent and non-adjacent elements in y-polarization, respectively. Meanwhile, the $S_{9,11}$, $S_{13,11}$, and $S_{25,11}$ are the mutual couplings between the adjacent

and non-adjacent elements in x-polarization, respectively. The configurations of $S_{11,11}$, $S_{12,11}$, and the rest S-parameters illustrate that the -24 dB decoupling bandwidth of the arrays is 4.21-4.79 GHz.

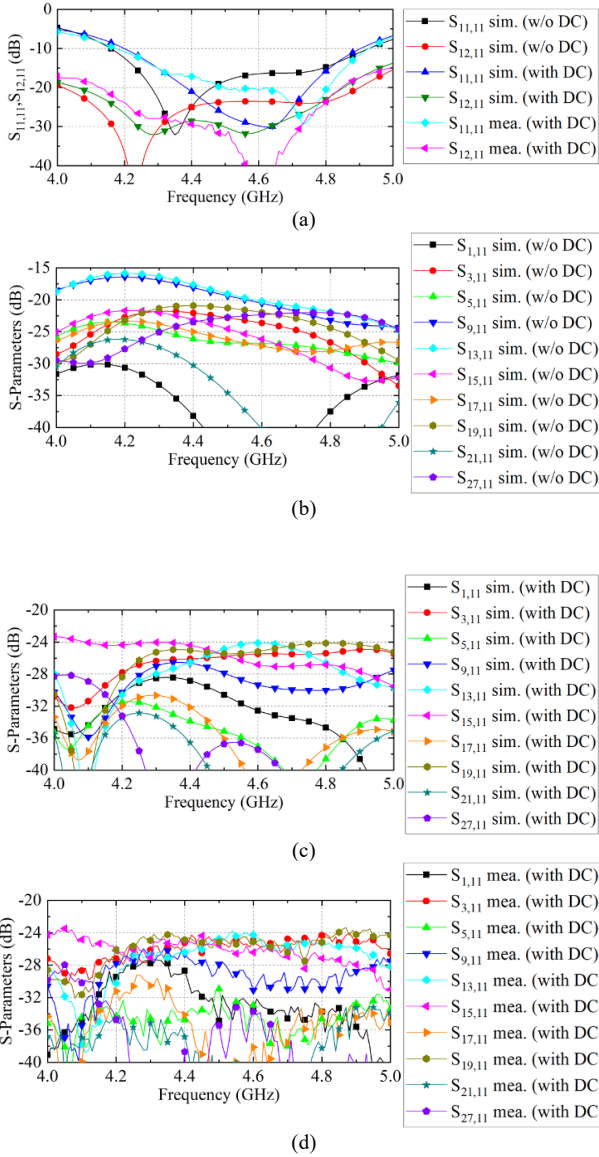


Fig. 3. The simulated and measured S-parameters of arrays with and without DCIM: (a) $S_{11,11}$ and $S_{12,11}$, (b) Simulated S-parameters of the array without DC, (c) Simulated S-parameters of the array with DC, (d) Measured S-parameters of the array with DC.

The simulated and measured radiation patterns of the array elements in the E-plane and H-plane at 4.3 GHz, 4.5 GHz, and 4.7 GHz are selected and shown in Fig. 4. It shows that the radiation patterns with decoupling in the E plane have amelioration to a certain degree. But the slightly deterioration occurs in the H plane at 60° and 315° . There is a trade-off between the patterns in the E-plane and H-plane. Besides, the radiation patterns in the H plane are also broader than those without decoupling, which will enhance the large angle scanning property of the array. In addition, the cross-polarized level of the array in the E-plane and H-plane is relatively high, which is caused by the engraved slot along $\pm 45^\circ$ on the patches, thereby a current distribution along $\pm 45^\circ$ is generated that

contributes to the deterioration of the x-pol level. Due to the radiation patterns cannot be cut with a plane in every direction. Thus, the radiation patterns are usually cut in E-plane and H-plane for the convenience of observation. Although the x-polarization level observed in E-plane and H-plane is higher than -20 dB, the x-polarization level can reach an ideal level in other cutting planes.

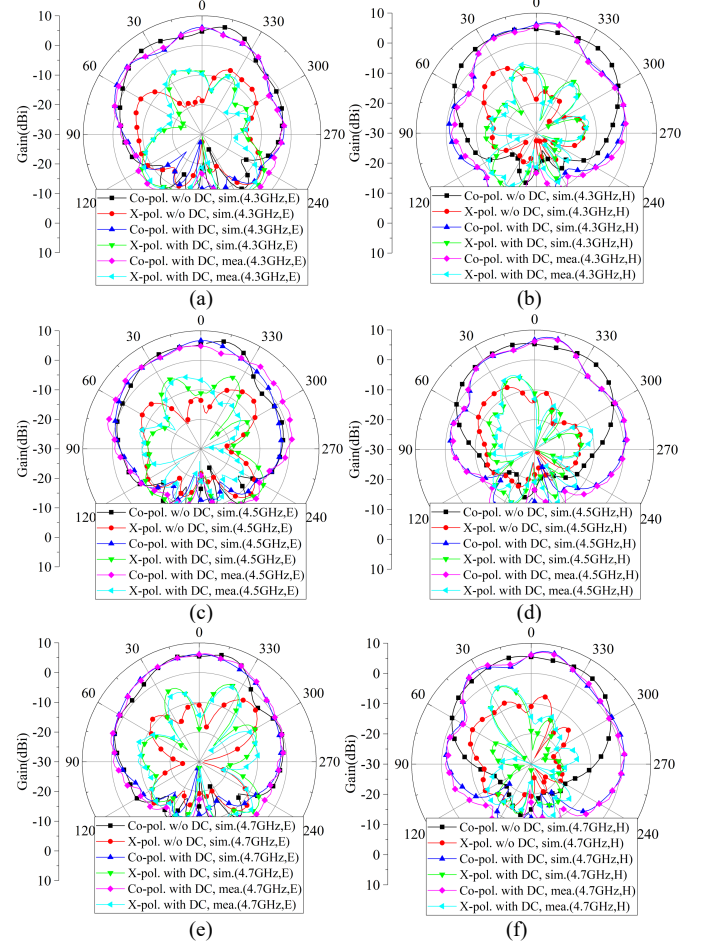


Fig. 4. The radiation patterns of the arrays with and without DC: (a) E-plane of port 1 at 4.3GHz, (b) H-plane of port 1 at 4.3GHz, (c) E-plane of port 1 at 4.5GHz, (d) E-plane of port 1 at 4.5GHz, (e) E-plane of port 1 at 4.7GHz, (f) H-plane of port 1 at 4.7GHz

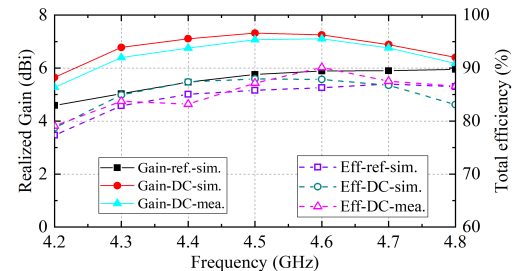


Fig.5 The realized gain and total efficiency of the array with and with DC.

Fig. 5 presents the realized gain and the total efficiency of the arrays with and without DC, respectively. When the DC is placed on the top surface of the array, the effective radiation area of the microstrip antenna is enlarged to all the cross-section of the DC unit. Therefore, the microstrip antenna with DC has a larger radiation aperture. The antenna gain is improved by mounting the DC. Consequently, both the realized gain and

total efficiency have significant increments by using DC. During the progress of designing a MIMO transmission system, the mutual coupling effect must be alleviated to avoid high active VSWR at transmitter ports. The ECC is another indicator to measure the decoupling performance of the array as well. Here, the simulation results of ECC with and without decoupling are lower than 0.003. Thus, the ECC between the excitation ports is not the main issue, which is not shown in this paper due to the length limitation.

III. ANALYSIS OF PARAMETERS STUDY AND DECOUPLING MECHANISM

A. Parametric study

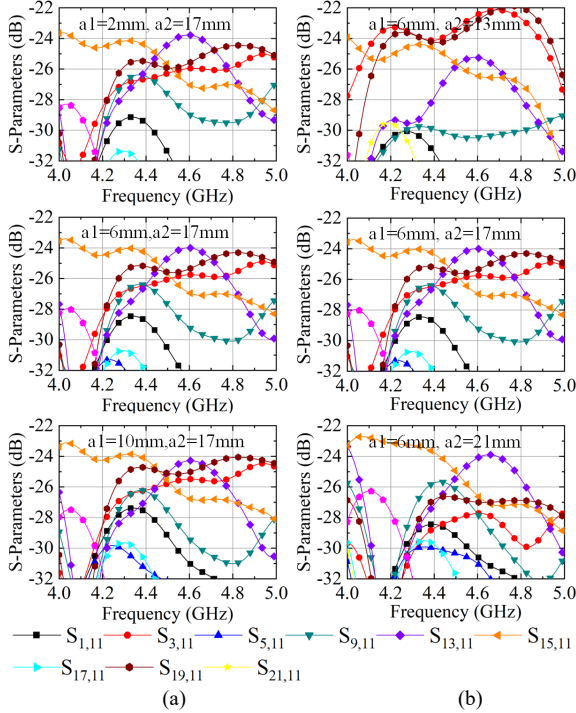


Fig.6 The S-parameters of the array with DC, (a) different a_1 as a_2 is 17mm, (b) different a_2 as a_1 is 6mm.

The sizes a_1 and a_2 of the air cavity determine the decoupling performance of the 4×4 arrays. Parametric studies for the overall array with DC have been carried out to illustrate the effect of the a_1 and a_2 on the decoupling level. Fig. 6 (a) and Fig. 6 (b) give the S-parameters with different a_1 and a_2 , respectively. The same S-parameters are selected as the above-mentioned ones in the last section. It can be found that when a_1

is 6 mm and a_2 is 17 mm, the lowest coupling is obtained within the working band (lower than -24 dB), which means the highest insertion loss is got in the tangential direction of the DC. But when a_1 and a_2 are set as other values, the S-parameters is higher than -24 dB. The simulated results also illustrate that a_1 and a_2 play the fine-tuning and decisive roles during the progress of decoupling for the 4×4 arrays, respectively.

B. E-fields

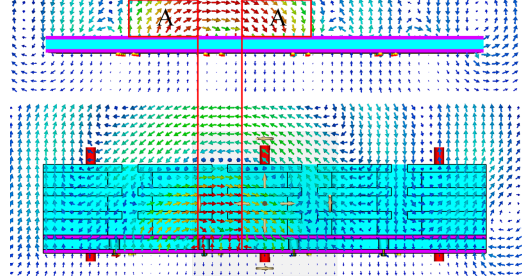


Fig.7 The E-fields of the 4×4 arrays with and without DC.

To better understand the decoupling mechanism of the proposed DC, the E-field distributions of the 4×4 arrays with and without DC in H-plane are presented in Fig. 7. By comparing the E-fields of the array with and without DC, it shows that when there is no DC on the top surface of the array, the E-field in the region A is very strong, which means the strong space waves coupling component propagates to the neighboring elements. While the DC is loaded, the E-field in the same position is extremely weak and constrained in the DC, where fewer space waves coupling component can propagate through the DC. The E-field in E-plane has a similar result with that in H-plane. All the results provide a vision proof that the proposed DC can effectively suppress the propagation of the main coupling component.

According to the parametric study and E-field of the array with and without DC prementioned above, the design criterion of the DC can be concluded as here. The DC unit consists of two layers of pure PP boards stacked together. Two air cavities are etched on the pp boards to form a DC. First, the cavities on the bottom and top layers of PP boards have the same dimensions. Then, the envelope of the S-parameter, lower than -24 dB, can be carried by varying the cavity sizes of the a_2 and a_1 in order. It should be noted that the air cavity in the bottom substrate should have a larger size than the radiation patches so that the propagation of the space waves coupling along the tangential direction of the array can be effectively suppressed.

TABLE II
PERFORMANCES COMPARISON

Ref.	[14]	[16]		[17]	[18]	This work
Method	ADS	Near-field resonator		DG	Embed. structure	DC
Frequency (GHz)	3.2-3.9 (19.7%)	2.38-2.53 GHz (6.1%)	2.38-2.49 GHz (4.5%)	4.9-5.2 (5.9%)	3.3-4.5 (30.8%)	4.21-4.79 (12.9%)
Height (λ_0)	0.40 λ_0	0.05 λ_0		0.25 λ_0	0.31 λ_0	0.45 λ_0
Inter-element distance (λ_0)	0.65 λ_0 , 0.40 λ_0	0.47 λ_0		0.62 λ_0	0.56 λ_0	0.5 λ_0
Total efficiency	NG	NG		>90%	80%	>80%
X-polarization	>10	>9		>10	>10	>7
Gain (dBi)	8.0	4.45		7.3	6.5	7.9
Isolation	25	20		24.5	20	24
Pot. for wider-b. and low x-pol.	no	no		no	no	yes
Toler., cost, and complex. of fab.	high	high		high	high	low

Embed.: Embeddable Pot.: Potential x-pol.: x-polarization Toler.: Tolerance Complex.: Complexity fab.: fabrication

IV. COMPARISON

A comprehensive comparison between the proposed decoupling technology of DC and the current literature for massive MIMO arrays is made and listed in TABLE II. It is observed that the inter-element distance of the arrays in [14] and [17] are relatively large. Furthermore, the isolation of these arrays does not have a prominent increment. In addition, though the decoupling structure proposed in [14] and [18] has a rather wide bandwidth, they have high design and fabrication complexity. The near-field resonator is a novel decoupling concept, but it has a narrow working band, and its isolation can only be enhanced to 20 dB. The antenna height is not the most important index in the actual application. Therefore, although the array in our work has the highest profile, its effect can be neglected. In addition, on the basis of ensuring the requirements of the wideband operating band, the array in our work has relatively high total efficiency. The gain of our work is comparable with that in [14] and higher than in [16], [17], and [18]. The cross-polarization level in our work is higher than the rest arrays, but it is caused by the inherent defects of the antenna unit itself. An array with a low cross-polarization level and wider bandwidth can be got by replacing the original array element with one that has improved performance. The complexity and the cost of the fabrication for the industrial application is important. The DC proposed in this paper only needs to be mounted on the top surface of the array without any air gap, which almost does not introduce deformation. PP and other low-permittivity materials are common in the market and easy to obtain. Obviously, the proposed decoupling concept has the best fabrication tolerance, complexity, and cost. In conclusion, the array with DC has an overall high performance and industrial application value compared with the others in current literature. Besides, it is worth noting that the proposed DC is mainly used to suppress the space waves coupling component. This method is general and can be used for the planar array antennas with other kinds of elements, such as monopole and dipole antennas, making it as a promising candidate for the wireless communication systems.

V. CONCLUSION

This letter developed a concept of DC for massive MIMO arrays. The decoupling mechanism was analyzed in detail. A DC element was proposed with an air cavity engraved on it to raise the transmission in the normal direction and the insertion loss characteristics in the tangential direction of the DC. The 4×4 massive MIMO array was simulated, fabricated, and measured. The results illustrate that the DC can effectively enhance the isolation of the array to more than 24 dB within the bandwidth of 4.21–4.79 GHz. In addition, the realized gain and the total efficiency of the array with DC have a significant increment. [The parametric study and E-field of the array before and after decoupling are given to provide a basic design criterion.](#) Furthermore, the proposed decoupling method has the potential of being applied in other array types, such as monopole and dipole arrays.

VI. REFERENCE

- [1] À. O. Martínez, J. Ø. Nielsen, E. D. Carvalho, and P. Popovski, "An experimental study of massive MIMO properties in 5g scenarios," *IEEE Trans. Antennas Propag.*, vol. 66, no. 12, pp. 7206–7215, Dec. 2018.
- [2] G. R. Nikandish, G. R. Nikandish, A. Zhu, "A fully integrated gan dual-channel power amplifier with crosstalk suppression for 5G massive MIMO transmitters," *IEEE Trans. on circ. and syst. II: expr. brie.*, vol. 68, no. 1, pp. 246–250, Jun. 2021.
- [3] X. Chen, S. Zhang, and Q. Li, "A review of mutual coupling in MIMO systems," *IEEE Access*, vol. 6, pp. 24706–24719, 2018.
- [4] O. Saatlou, M. O. Ahmad, and M. N. S. Swamy, "Spectral efficiency maximization of multiuser massive MIMO systems with finite-dimensional channel via control of users' power," *IEEE Trans. on circ. and syst. II: expr. brie.*, vol. 65, no. 7, pp. 883–887, Jul. 2018.
- [5] O. Castañeda, S. Jacobsson, G. Durisi, T. Goldstein, and C. Studer, "High-bandwidth spatial equalization for mm wave massive MU-MIMO with processing-in-memory," *IEEE Trans. on circ. and syst. II: expr. brie.*, vol. 67, no. 5, pp. 891–895, May. 2020.
- [6] A. Zhang, W. Cao, P. Liu, J. Sun, and J. Li, "Channel Estimation for MmWave Massive MIMO With Hybrid Precoding Based on Log-Sum Sparse Constraints," *IEEE Trans. on circ. and syst. II: expr. brie.*, vol. 68, no. 6, pp. 1882–1886, Jun. 2021.
- [7] X. Tan, W. Wang, Y. Wu, Y. Liu, and A. A. Kishk, "Enhancing isolation in dual-band meander-line multiple antenna by employing split EBG structure," *IEEE Trans. Antennas Propag.*, vol. 67, no. 4, pp. 2769–2774, Apr. 2019.
- [8] W. Wang, Y. Wu, W. Wang, and Y. Yang, "Isolation enhancement in dual-band monopole antenna for 5G applications," *IEEE Trans. on circ. and syst. II: expr. brie.*, vol. 68, no. 6, pp. 1867–1871, Jun. 2021.
- [9] C. Tang, X. Chen, T. Shi, H. Tu, Z. Wu, and R. W. Ziolkowski, "A compact, low-profile, broadside radiating two-element huygens dipole array facilitated by a custom-designed decoupling element," *IEEE Trans. Antennas Propag.*, vol. 69, no. 8, pp. 4546–4557, Aug. 2021.
- [10] Z. Qamar, U. Naeem, S. A. Khan, M. Chongcheawchamnan, and M. F. Shafique, "Mutual coupling reduction for high-performance densely packed patch antenna arrays on finite substrate," *IEEE Trans. Antennas Propag.*, vol. 64, no. 5, pp. 1653–1660, May. 2016.
- [11] Y. Zhu, Y. Chen, and S. Yang, "Helical Torsion Coaxial Cable for Dual-Band Shared-Aperture Antenna Array Decoupling," *IEEE Trans. Antennas Propag.*, vol. 68, no. 8, pp. 6128–6135, Aug. 2020.
- [12] F. Liu, J. Guo, L. Zhao, G. Huang, Y. Li, and Y. Yin, "Dual-band metasurface-based decoupling method for two closely packed dual-band antennas," *IEEE Trans. Antennas Propag.*, vol. 68, no. 1, pp. 552–557, Jan. 2020.
- [13] M. Li, M. Y. Jamal, L. Jiang, and K. L. Yeung, "Isolation Enhancement for MIMO Patch Antennas Sharing a Common Thick Substrate: Using a Dielectric Block to Control Space-Wave Coupling to Cancel Surface-Wave Coupling," *IEEE Trans. Antennas Propag.*, vol. 69, no. 4, pp. 1853–1863, Apr. 2021.
- [14] K. Wu, C. Wei, X. Mei and Z. Zhang, "Array-antenna decoupling surface," *IEEE Trans. Antennas Propag.*, vol. 65, no. 12, pp. 6728–6738, Dec. 2017.
- [15] Y. Zhang, S. Zhang, J. Li, and G. F. Pedersen, "A Transmission-Line-Based Decoupling Method for MIMO Antenna," *IEEE Trans. Antennas Propag.*, vol. 67, no. 5, pp. 3117–3131, May. 2019.
- [16] M. Li, B. G. Zhong, and S. W. Cheung, "Isolation enhancement for MIMO patch antennas using near-field resonators as coupling-mode transducers," *IEEE Trans. Antennas Propag.*, vol. 67, no. 2, pp. 755–764, Feb. 2019.
- [17] S. Zhang, X. Chen, and G. F. Pedersen, "Mutual coupling suppression with decoupling ground for massive MIMO antenna arrays," *IEEE Trans. Veh. Technol.*, vol. 68, no. 8, pp. 7273–7282, Aug. 2019.
- [18] Y. Qin, R. Li, and Y. Cui, "Embeddable structure for reducing mutual coupling in massive MIMO antennas," *IEEE Trans. Access*, vol. 8, pp. 195102–195112, Oct. 2020.
- [19] M. Li and S. Cheung, "Isolation Enhancement for MIMO Dielectric Resonator Antennas Using Dielectric Superstrate," *IEEE Trans. Antennas Propag.*, vol. 69, no. 7, pp. 4154–4159, Jul. 2021.